Grating Scatter in the HST Faint Object Spectrograph

Cindy C. Cunningham and John Caldwell

Space Astrophysics Laboratory
Institute for Space and Terrestrial Science
4850 Keele St.,
North York, ONT, M3J 3K1, Canada

ABSTRACT

We compare May, 1991 HST FOS and GHRS spectra of solar analog star 16 Cyg B (spectral type G2 V) with Space-Lab 2 SUSIM observations of the Sun (Van Hoosier *et al.* 1988), and with earlier 16 Cyg B observations by the IUE. Grating scatter significantly affects the FOS spectra below 2100Å wavelength. Below 1800Å, a GHRS G140L ("solar blind") spectrum of 16 Cyg B shows no evidence of grating scatter. This spectrum may therefore be used to verify the accuracy of corrections to FOS G190H spectra of solar–like objects, ranging from galaxies to planets. Between 1750Å and 2100Å, the recommended correction to FOS spectra is a simple background subtraction from the HST "counts file". Below $\sim$ 1700Å, FOS spectra of solar–like objects contain no information. Additional FOS observations of several red objects which had been observed by the GHRS G140L before the Side 1 electronic failure, are planned.

ACRONYMS

HST = Hubble Space Telescope

FOS = Faint Object Spectrograph

GHRS = Goddard High Resolution Spectrograph

SUSIM = Solar Ultraviolet Spectral Irradiance Monitor

IUE = International Ultraviolet Explorer

G140L, G200M, G270M = gratings in the GHRS with respective "central" wavelengths of 1400, 2000 and 2700Å

G190H, G270H = gratings in the FOS with respective central wavelengths of 1900 and 2700Å

October 18, 1993

This is a semi-final draft of a manuscript to be submitted for publication after a workshop at the Space Telescope Science Institute, November 15, 1993.

INTRODUCTION

The original motivation for obtaining the spectra reported here was to measure instrumentally scattered, long–wavelength light within the FOS during observations of red objects. This was to be accomplished by comparing nearly simultaneous observations of a common target with both the FOS and the GHRS. The goal was to see if the FOS G190H grating, of which the detector is specifically designed to be sensitive to photons from the visible to the ultraviolet, could be corrected so that it would reliably overlap with the GHRS G140L grating. G140L is sensitive only to ultraviolet photons, specifically because of its detector design. Reference to this GHRS characteristic is commonly stated as being "solar–blind".

The GHRS has two independent electronic "sides". The G140L grating is on side 1, which has a CsI photocathode. It is extremely insensitive to light at wavelengths longer than 1800Å. GHRS gratings G200M and G270M are on side 2, with a CsTe photocathode that is sensitive up to 3200Å. G200M spectra of red objects below 2000Å could therefore in principle have been somewhat susceptible to grating scatter of near–ultraviolet photons, but this concern did not prove to be serious.

The FOS also has two independent sides, which cover the same spectral range. The FOS "red" detector is everywhere more sensitive than the "blue" one at all wavelengths, including visible. The red detector is therefore more susceptible to grating scatter than the blue, for which reason the blue side was chosen for these observations.

On 27 May, 1991, the G2V star 16 Cyg B was observed by both the FOS and the GHRS. This star was chosen because it is an HST ultraviolet standard star and because it resembles the Sun very closely in ground-based spectra (Hardorp, 1978). The solar similarity permits an independent verification of HST instruments with respect to grating scatter, through comparison with published solar ultraviolet observations. The HST observations are summarized in Table I.

It had been anticipated, and it has been verified herein, that a correction to FOS G190H spectra is necessary to provide an efficient means of covering its spectral range, from 1600 to 2300Å, for red objects. However, with the subsequent loss of side 1 of the GHRS, the usefulness of the FOS G190H for red objects has become even more critical, and systematic techniques to minimize the effects of grating scatter are required.

TABLE I.

		"Side"	Spectral Range or central wavelength	Exposure time
FOS	G190H	Blue	1570 - 2330Å	31.5M
	G270H	Blue	2230 - 3300Å	5.2M
	G160L	Blue	1150 - 2520Å	8.4M
GHRS	G140L	1	1560 - 1840Å 1700Å center	68.6M (total = 68.6M)
	G270M	2	24 settings, 2300 - 3220Å centers	96.0S - 6.4S (total = 10.96M)
	G200M	2	12 settings, 1800 - 2185Å centers	26.6M - 4.2M (total = 176.6M)

ANALYSIS

It was first necessary to harmonize the wavelength sampling of the two spectrographs, prior to the intercomparison. Each spectrum is originally oversampled, with multiple samples per Å. In each case, the data were resampled on 0.5Å centers, with the resampled value being a weighted mean over ±0.5Å, with a weight of 1.0 at the sample center, decreasing linearly to zero at ±0.5Å.

The GHRS data were then composited into a single spectrum covering the range 1600 – 3300Å. The "solar blind" G140L spectrum of 16 Cyg B was first compared to the G200M spectra that overlapped it in wavelength (Figure 1). It is evident from this figure that there is little or no grating scatter evident in the GHRS spectra obtained with the side 2 CsTe photocathode detector. The continua of the two gratings are in excellent agreement. The differences in the two Si II emission lines at 1808 and 1817Å are greater than the noise in the continuum, so this is probably a detection of temporal variability in the stellar chromospheric emission.

GHRS exposure times had originally been calculated with the expectation of binning data to lower spectral resolution during analysis, to improve signal-to-noise. It would have been prohibitive to obtain high signal-to-noise per diode for the GHRS. Indeed, this realization was part of the original motivation for extending the useful wavelength range of the FOS G190H as far shortward as possible, well before the failure of GHRS side 1 electronics was ever contemplated. For the following comparison between spectrographs,

GHRS spectra have therefore been further smoothed with a boxcar filter over 9 resampled points, ±2.0Å.

When the reduced FOS and GHRS data are compared, it is apparent that there is a discrepancy between the two with respect to absolute calibration. This has been resolved by comparison with IUE observations of 16 Cyg B. The IUE data have much lower spectral resolution, but the absolute flux calibration is considered to be reliable. Figure 2 compares the ratios FOS/IUE and GHRS/IUE in a region of the spectrum where grating scatter is not expected to be significant. (This expectation is confirmed below.) The two HST spectra agree quite well with each other qualitatively, but only the FOS data agree quantitatively with the IUE. However, as shown in Figure 2, after a constant factor of 0.91 has been applied to each point in the GHRS data, the two HST spectra also agree quantitatively with each other to high precision. This factor will be included in all subsequent discussion of GHRS data herein.

The reason why this absolute calibration correction is necessary is as follows. All HST spectral data reach the astronomical user through a processing system known informally as the "pipeline". At the time these data were obtained, FOS pipeline data were routinely corrected for light loss due to spherical aberration, while the GHRS data were not. Thus, a normalization factor must be applied to the GHRS data.

Figure 3a compares FOS and GHRS 16 Cyg B spectra with solar data obtained in 1985 in the Space-Lab 2 SUSIM experiment (Van Hoosier *et al.* 1988). The FOS spectrum in its uncorrected form clearly exhibits significant grating scatter at short wavelengths with respect to the other two spectra. The scatter becomes apparent near $\sim$ 2100Å, and increases rapidly at shorter wavelengths.

Correcting this scatter is the main goal of this paper. In Figure 3b, we show a corrected version of the spectrum from Figure 3a, to demonstrate the magnitude of the effect. The low wavelength (1600-2200Å) region where the correction to the FOS data is most significant is emphasized in Figure 3b. The details by which the correction is made will be described below. However, we first briefly describe some additional features of the data which have influenced our work.

There are two reasons why grating scatter in the FOS causes the apparent flux in the FOS spectrum to deviate from the other two spectra below 2100Å in Figure 3a. The first is that, as the true signal decreases rapidly, the excess scattered light, which is approximately grey, becomes relatively more important. The second is that the decreasing sensitivity of the FOS toward shorter wavelengths enhances the excess in the flux calibration process.

The FOS spectrum (corrected for grating scatter) and the GHRS spectrum (corrected by a constant factor of 0.91, as described above) are shown in Figure 3b to be nearly identical down to about 1760Å. Note that the Si II emission lines clearly evident at 1808 and 1817Å in the GHRS data in both Figures 3a and 3b. The lines are suppressed somewhat by the instrumentally enhanced background of the FOS in Figure 3a, with its semi-log scale, but they are clearly seen to be comparable in both the corrected and uncorrected FOS spectra in Figure 3b (with linear axes). At a few other wavelengths, the agreement

is not as good, but that may be due simply to noise in the data.

Figure 4 shows the ratios of the FOS (grating scatter corrected) and GHRS spectra of 16 Cyg B and SUSIM solar spectra. Input data for the ratios were taken directly from Fig. 3a, but after the ratio was performed, the data were further binned to 8Å. There is a significant difference in the range 1800 – 2300Å between the stellar spectra as measured by both HST spectrographs and the solar spectrum. The difference is consistent with a small difference in effective temperature between the two stars, in the sense that 16 Cyg B has a slightly cooler effective temperature than the Sun. Since the difference becomes apparent at 2300Å, a wavelength where the Sun is known to exhibit only very small temporal variations, it is probably not a temporal effect associated with the solar cycle or its stellar analog.

Since all of the criteria by which 16 Cyg B was determined to be a solar analog were applied at wavelengths above 3000Å (Hardorp, 1978), and since stellar radiation becomes exponentially more sensitive to temperature toward shorter wavelengths, it is not surprising that the two stars should eventually diverge in brightness.

Having considered these characteristics in the data with which the FOS is being compared, we now return to the primary topic – correcting the FOS by using the imperfect comparison data to remove the background due to grating scatter.

All HST spectral data from the pipeline comes in three forms: raw "counts", which is essentially the unprocessed telemetry from the spacecraft; calibrated counts, which includes quantum efficiency effects and other corrections such as interpolations across bad detector diodes; and a flux file, which includes the throughput sensitivity function.

The level for the FOS G190H grating scatter correction is determined by calculating the average value in the calibrated counts spectrum (FOS file extension - c5h) over the wavelength range from 1575Å – 1700Å. By inspection, the calibrated counts over this range are approximately constant with wavelength, which is not physically plausible for a G2V star, but which is quite plausible for typical grating scatter. Further, a pre-launch calibration measurement of grating scatter in the FOS (Blair *et al.*) is also consistent with its being approximately constant with wavelength. The average value, 0.54 for the 16 Cygni B FOS G190H spectrum, is then subtracted from each datum in the counts file.

The final step in obtaining the corrected flux spectrum of the star is to multiply the corrected, calibrated counts file by the spectral sensitivity function of the FOS. This function is not routinely available from the data, but it may be accurately represented by the ratio of the original flux spectrum from the pipeline to the original, uncorrected counts spectrum from the pipeline. The result is the FOS spectrum in flux units. For 16 Cyg B, the final product is shown as the corrected FOS spectrum in Figure 3b.

The corrected spectrum is clearly not perfect in this case. In Figure 3b, it is evident that the "corrected " curve is actually slightly negative near 1700Å. This indicates that a slightly more sophisticated approximation to the scattered light component might be useful, and this will be discussed below. Before doing that, however, we describe how grating scatter affects the FOS G270H.

G270H data are corrected in a manner similar to that for G190H. The background level that is subtracted from the G270H calibrated counts file is set by scaling the G190H scattered light count to the ratio of the G190H to the G270H counts in the spectral overlap region (2225 - 2325Å). For 16 Cygni B, the background value for the G270H grating was 0.63. The data were then rebinned using the resampling technique described above. Finally, G190H and G270H data in the region of overlap were averaged to create the FOS composite spectrum.

We now return to the question of a more formally exact representation of the scattered light curve, which can be derived in the ideal case that the GHRS data are completely free of systematic problems, including grating scatter and photon noise. The comparison between the G140L and G200M GHRS spectra (Figure 1) showed that within the limitations of the data these GHRS gratings are essentially free of grating scatter, but as discussed above, the data are not of high signal–to–noise.

In this ideal case, the only difference between the FOS and the normalized GHRS would be scattered light within the FOS. Subtracting the two curves then would give the scattered light spectrum within the FOS. The normalized GHRS flux may be converted from energy units to counts/second/diode using the inverse FOS calibration function. The results of such a calculation are shown in Figures 5a and 5b for the spectral range 1600 – 2100Å which was covered by the G140L and G200M gratings.

The FOS calibration function is determined by measurements of blue objects, in which photons near the wavelength of interest are not overwhelmed by orders of magnitude by photons at other wavelengths, so grating scatter is not a problem here.

The difference between the FOS pipeline count rate and the calculated scattered light count rate in Figure 5a would be the best estimate of the true 16 Cyg B signal in the FOS data, in the ideal case. By construction, if the difference between these two curves were converted to energy units, the calculated scattered light curve would be precisely the same spectrum as the GHRS G140L spectrum below 1840Å in Figure 3b. It might be considered that this derived curve could be used reliably to correct future FOS G190H observations of red objects. The procedure would be to scale the G190H planetary/stellar spectrum to the derived scattered light curve in Figure 5b near 1580Å, and subtract them. The difference would then be calibrated with the FOS calibration function, to produce a planetary/stellar spectrum for analysis. The confidence of the investigator in the quality of the result between 1600 and 1800Å would in large part be determined by the qualitative match between the simulated scattered light curve and the target observation at those short wavelengths where the true signal from the target could be assumed to be zero.

The question remains, however, whether or not this derived curve really would produce a more accurate correction to the data in the presence of noise than would a simple constant value background subtraction. Three different background estimates are shown in Figure 5b. The derived curve is very noisy above 1840Å as this is where the G140L GHRS data ends, and the signal to noise of the G200M data is quite low. The derived curve is actually quite well approximated by the constant value of 0.54 used above. A third curve, representing pre–launch laboratory measurements of FOS scattered light by

Blair *et al*, is also shown. There is little correlation in spectral detail between this curve and the derived background curve, suggesting that noise is significant.

One additional data set is available that is relevant to this background issue. Near simultaneous observations of Jupiter with both the FOS G190H and the GHRS G200M grating were made as part of Caldwell's GTO program. A scattered light background curve has been derived from these data. A comparison of this background curve to that derived from the 16 Cyg B observations is shown in Figure 6. The wavelength region covered by these data is restricted to the region from 1570 – 1800Å. A simplified composite between the curves derived from 16 Cyg B and Jupiter data is shown in Figure 7.

For a general application of this curve, the following procedure should be followed. The average value for the scattered light background should be calculated in the same manner as described previously. This value should be used at every point in the G190H spectrum except in the region from 1640 - 1760Å. From 1640 - 1680Å a linearly decreasing value should be subtracted, instead of the constant value used at other wavelengths. From 1680 - 1760Å a linearly increasing value should be subtracted instead of the constant value used at other wavelengths. The slope of the scattered light background curve from 1640 – 1680Å is equal to -0.00494 / (constant value determined from the counts file from 1570 – 1700Å) and similarly the slope of the background scatter curve from 1680 – 1760Å is 0.00296 / (constant value determined from the counts file from 1570 – 1700Å).

Using this procedure for correcting the FOS data will potentially push the believable lower wavelength limit to about 1700Å. Shortward of this wavelength FOS data of red objects cannot be easily corrected with existing scattered light observations.

REFERENCES

Blair, W. P., Davidsen, A. F., Uomoto, A. (1989). "Scattered Red Light in the FOS", unpublished, pre-launch FOS Calibration Report 058, Johns Hopkins University.

Hardorp, J. (1978) "The Sun Among the Stars. I. A Search for Solar Spectral Analogs", *A.A.*, **63**, 383–390.

Van Hoosier, M. E., J. F. Bartoe, G. E. Bruecker and D. K. Prinz, (1988), "Absolute Solar Spectral Irradiance 120nm - 400nm (Results from the Solar Ultraviolet Spectral Irradiance Monitor-SUSIM-Experiment on board Spacelab 2)", *Astro. Let. and Commun.*, **27**, 163-168.

FIGURE CAPTIONS

Figure 1: The overlap region between the GHRS G140L spectrum (solid line) of 16 Cyg B (side 1 - solar blind detector) and the 2 GHRS G200M spectra (dashed curve) (side 2 detector). Clearly there is little or no significant grating scatter in the G200M spectra.

Figure 2: Comparison of FOS and GHRS composite spectra. Both spectra are ratioed to a well calibrated IUE spectrum of 16 Cyg B. It is necessary to apply a multiplicative factor

of 0.91 to the GHRS/IUE ratio in order to bring the average value to 1.0. No scaling is necessary for the FOS spectrum. All data are rebinned with a 3Å wide triangular bin.

Figure 3a: Comparison of composite FOS and GHRS 16 Cyg B HST spectra with the solar SUSIM Space-Lab 2 ultraviolet spectrum by VanHoosier *et al.* (1988). The FOS spectrum is a composite of uncorrected G190H and G270H FOS observations described in Table I. A composite spectrum of all the GHRS spectra described in Table I is also plotted.

Figure 3b: The low wavelength segments of the corrected and uncorrected FOS composite 16 Cyg B spectra are shown and compared to the GHRS composite (additional boxcar smoothing of ± 1.0Å). A constant background correction (shown here) works well to correct the FOS grating scatter to about 1760Å.

Figure 4: The corrected FOS and GHRS composite spectra are ratioed to one another (A) and to the SUSIM solar spectrum (B and C) using input data taken directly from Figure 3a. After the ratio was performed, additional boxcar smoothing (± 4Å) was applied. FOS/solar (B) and GHRS/solar (C) agreements are good longward of 2300Å. In the range 1800 – 2100Å, the ratios depart from unity, probably because of real intrinsic differences between the Sun and 16 Cyg B. The FOS and GHRS data for curve A have been resampled with a 1Å wide triangular binning function. The GHRS data have additional boxcar smoothing ± 2Å and have been multiplied by 0.91. The FOS/GHRS ratio has had boxcar smoothing of ± 4Å applied. The FOS and solar data for curve B have been resampled with a 1Å wide triangular binning function. The solar data has additional boxcar smoothing ± 2Å and has been multiplied by 5e-14. The FOS/solar ratio has had boxcar smoothing of ± 4Å applied. The GHRS and solar data for curve C have been resampled with a 1Å wide triangular binning function. The solar data has been multiplied by 5e-14 and the GHRS data has been multiplied by 0.91. The GHRS/solar ratio has had boxcar smoothing of ± 4Å applied. Both the GHRS and the solar data have had additional boxcar smoothing ± 2Å

Figure 5a: A plot of the "simulated true" counts expected from 16 Cyg B as derived from the GHRS observations compared to the measured FOS counts.

Figure 5b: Possible backgrounds for correcting FOS grating scatter. A constant value is compared to a curve derived from a GHRS to FOS comparison and to pre-launch laboratory data by Blair *et al.*

Figure 6: The background curve derived from the GHRS and FOS observations of Jupiter is compared to that derived from the 16 Cyg-B observations.

Figure 7: The average of the Jupiter and 16 Cyg B background scatter curves is shown. This is formally the best curve for removing FOS grating scatter from G190H FOS observations, but it would be very risky to interpret results below 1700Å literally.

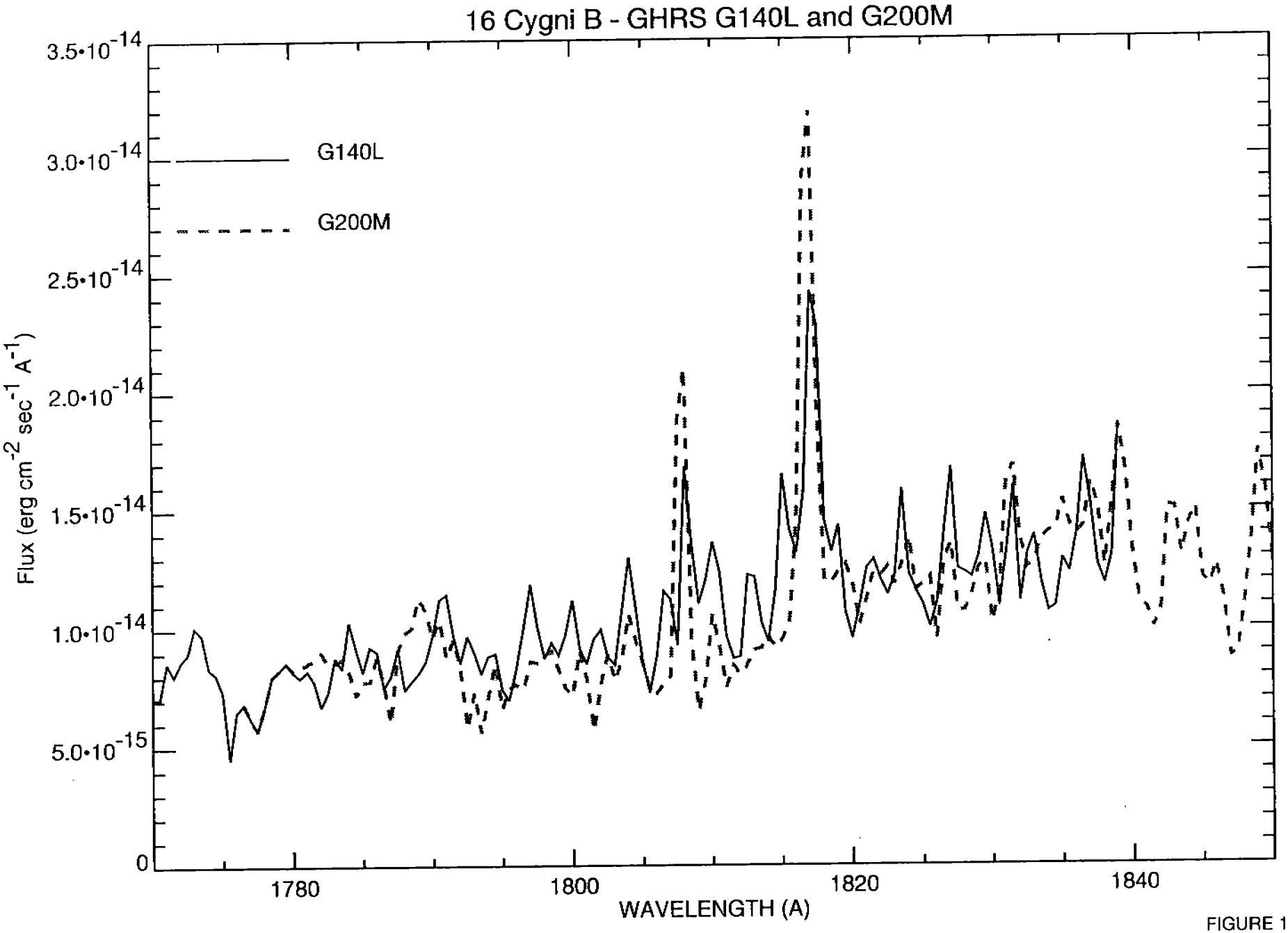
16 Cygni B - GHRS G140L and G200M
G140L
G200M
Flux (erg cm-2 sec-1 A-1)
3.5•10-14
3.0•10-14
2.5•10-14
2.0•10-14
1.5•10-14
1.0•10-14
5.0•10-15
0
1780
1800
1820
1840
WAVELENGTH (A)

FIGURE 1

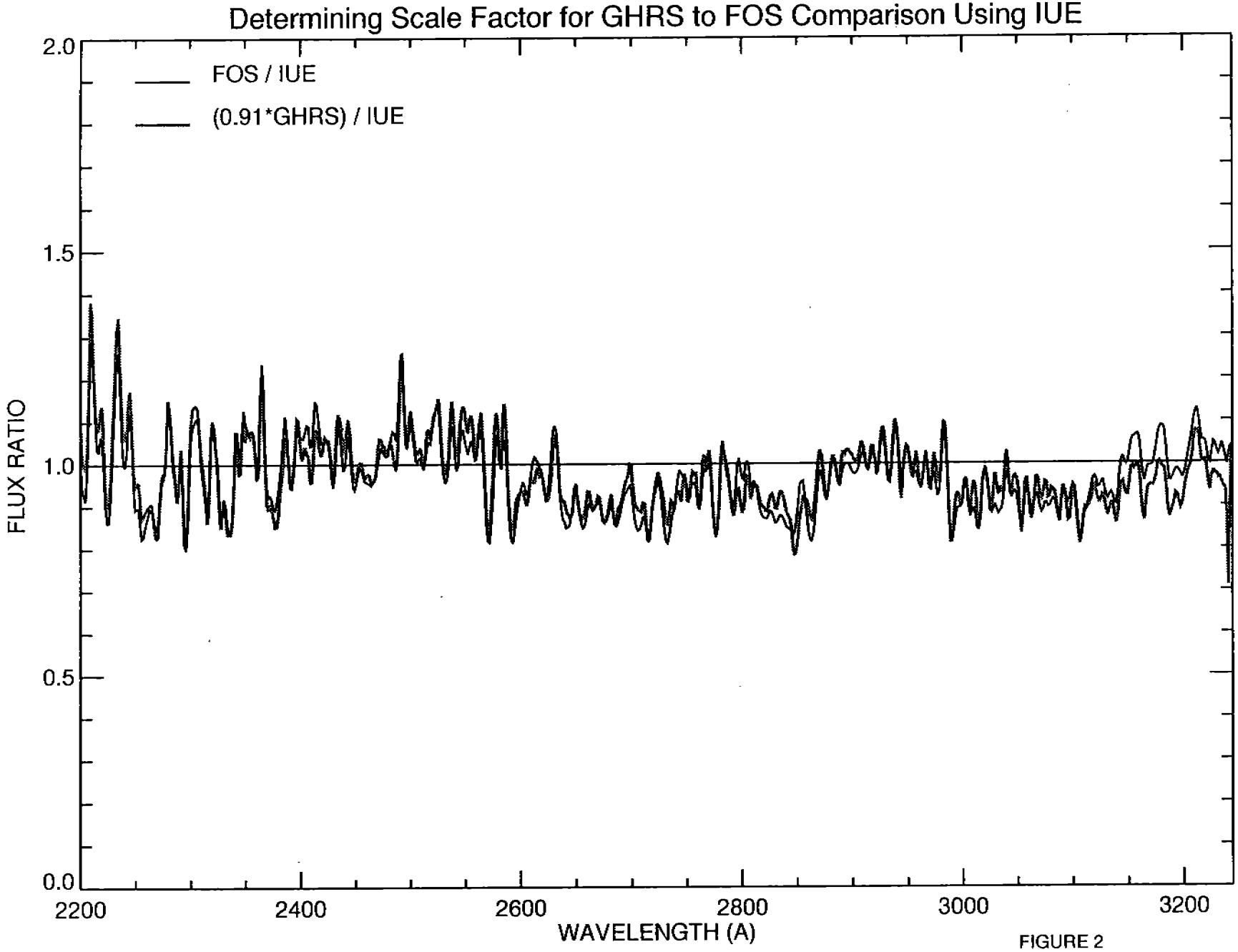
Determining Scale Factor for GHRS to FOS Comparison Using IUE
FOS / IUE
(0.91*GHRS) / IUE
FLUX RATIO
2.0
1.5
1.0
0.5
0.0
2200
2400
2600
2800
3000
3200
WAVELENGTH (A)

FIGURE 2

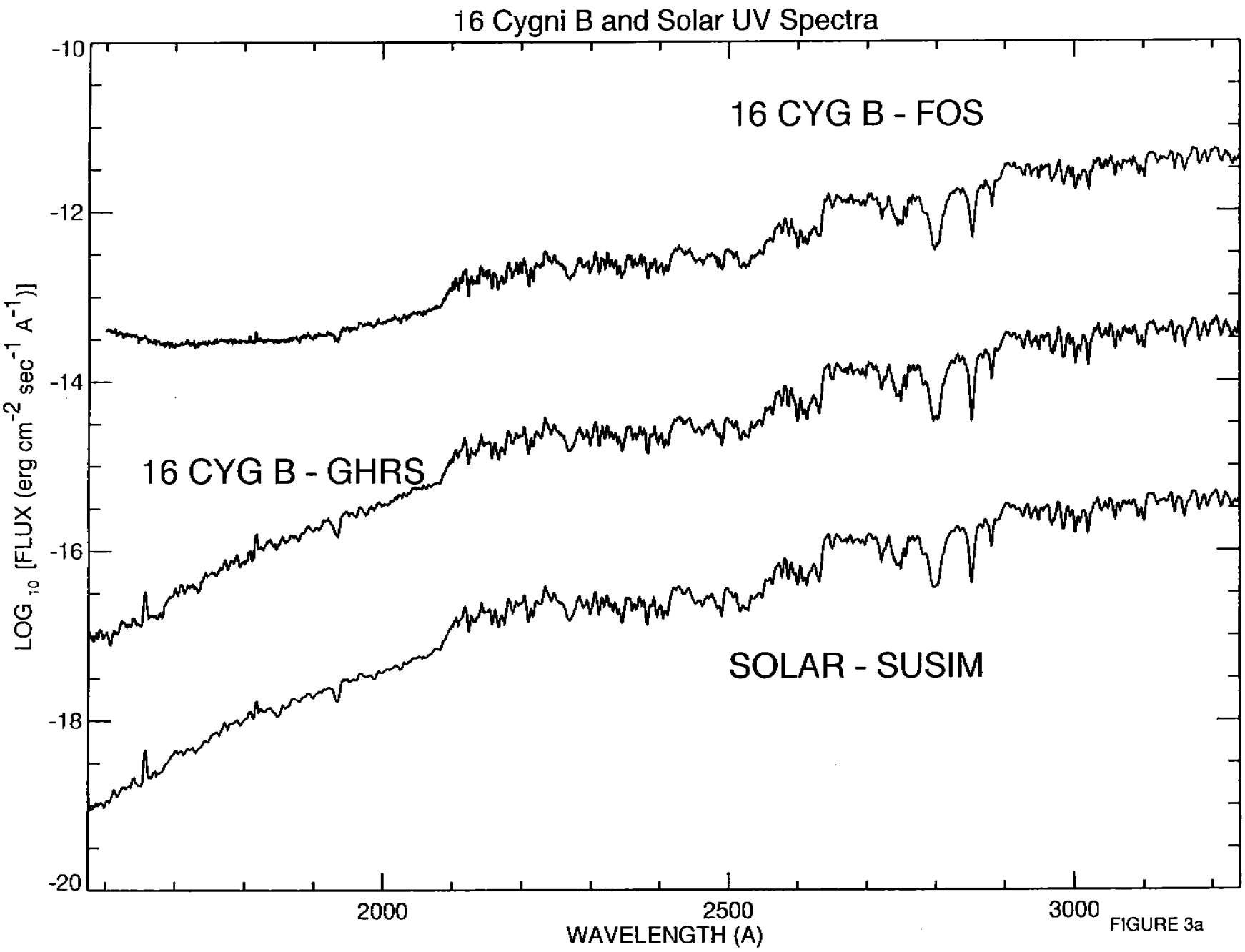
16 Cygni B and Solar UV Spectra
16 CYG B - FOS
16 CYG B - GHRS
SOLAR - SUSIM
LOG 10 [FLUX (erg cm-2 sec-1 A-1)]
WAVELENGTH (A)
-10
-12
-14
-16
-18
-20
2000
2500
3000

FIGURE 3a

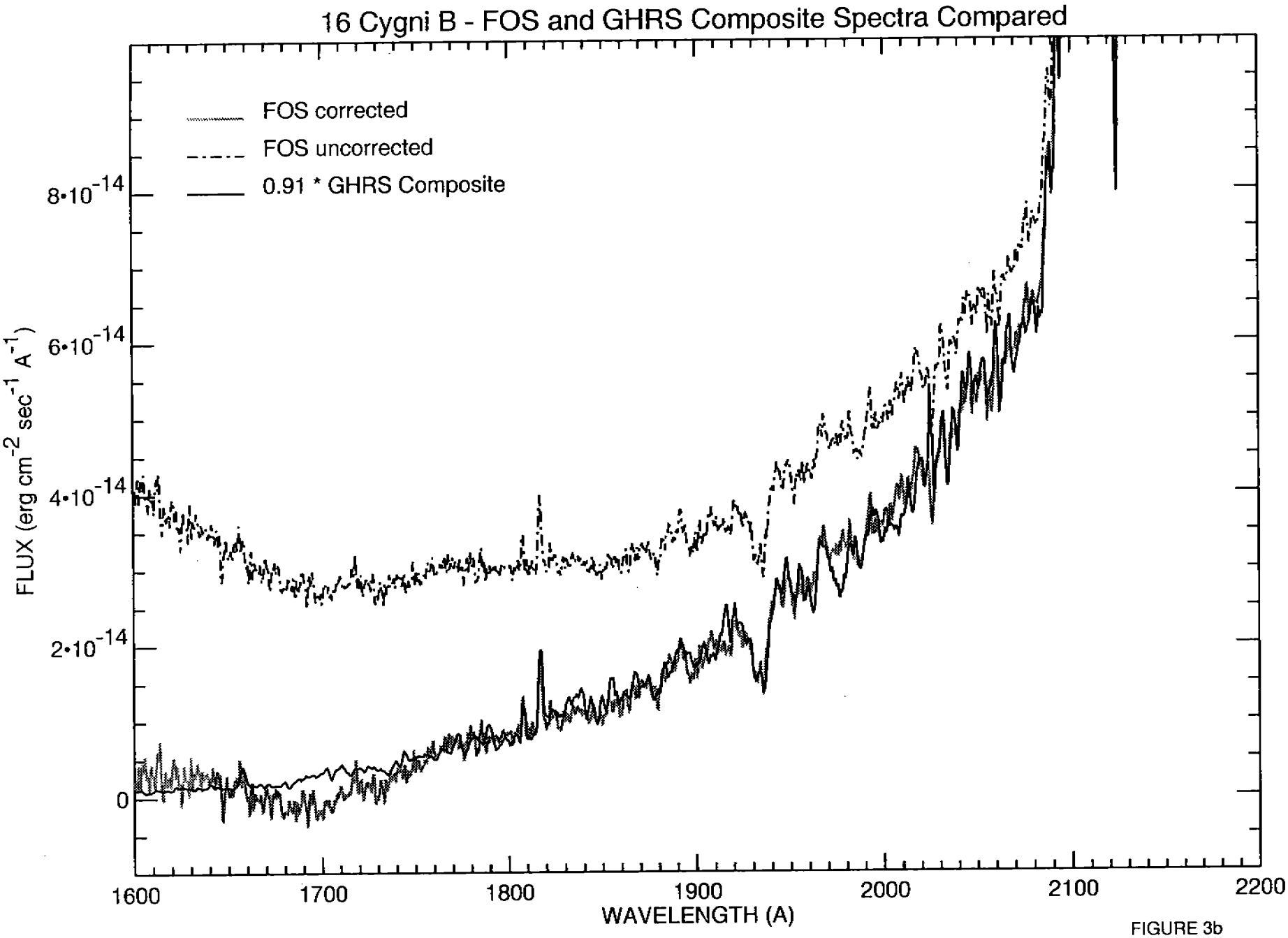
16 Cygni B - FOS and GHRS Composite Spectra Compared
FOS corrected
FOS uncorrected
0.91 * GHRS Composite
8•10^-14
6•10^-14
4•10^-14
2•10^-14
0
FLUX (erg cm^-2 sec^-1 A^-1)
1600
1700
1800
1900
2000
2100
2200
WAVELENGTH (A)

FIGURE 3b

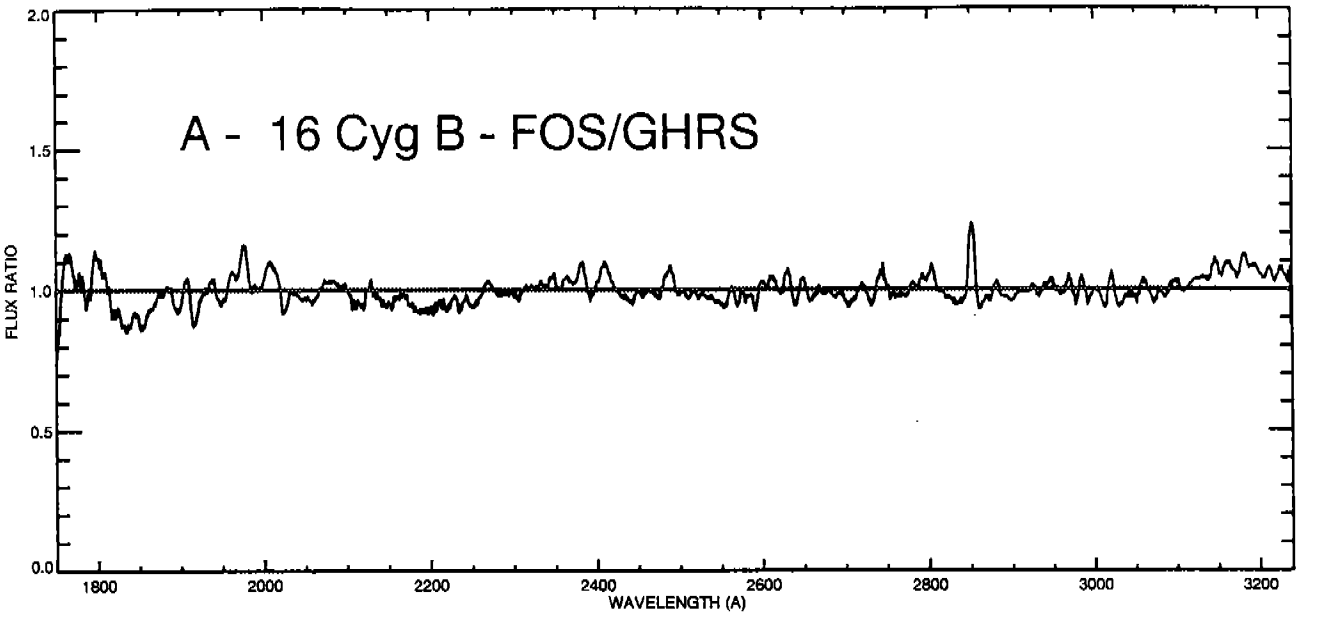
A - 16 Cyg B - FOS/GHRS
FLUX RATIO
WAVELENGTH (A)
2.0
1.5
1.0
0.5
0.0
1800
2000
2200
2400
2600
2800
3000
3200

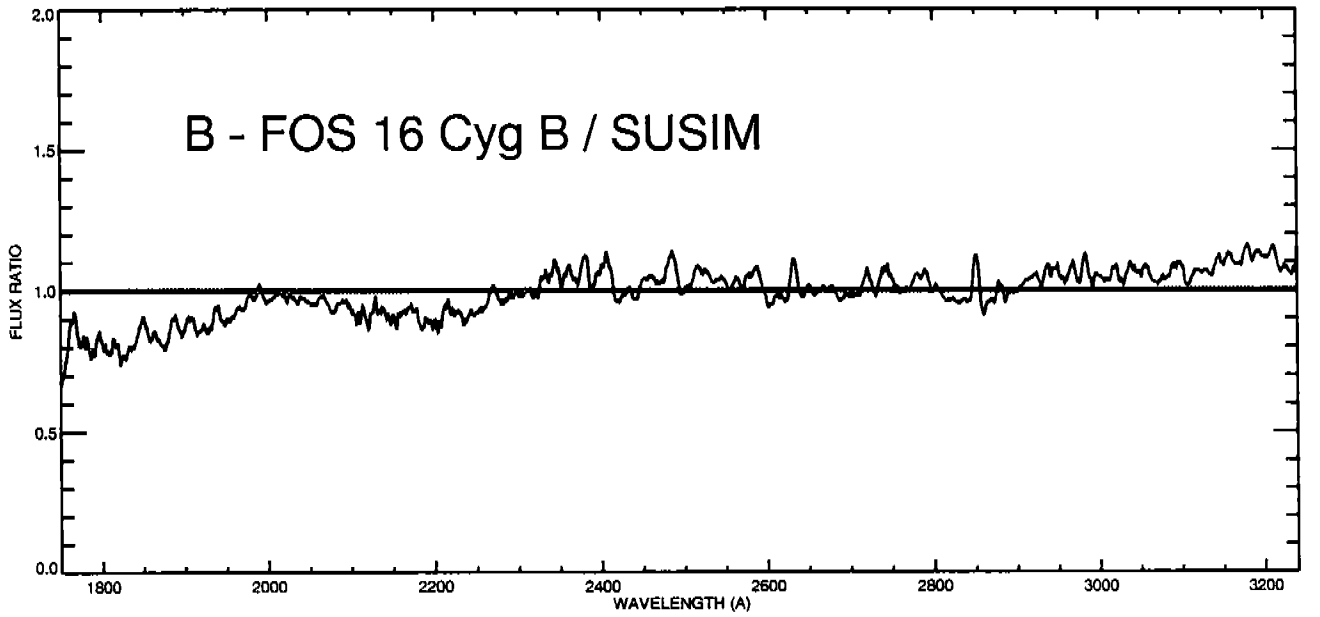
B - FOS 16 Cyg B / SUSIM
FLUX RATIO
WAVELENGTH (A)
2.0
1.5
1.0
0.5
0.0
1800
2000
2200
2400
2600
2800
3000
3200

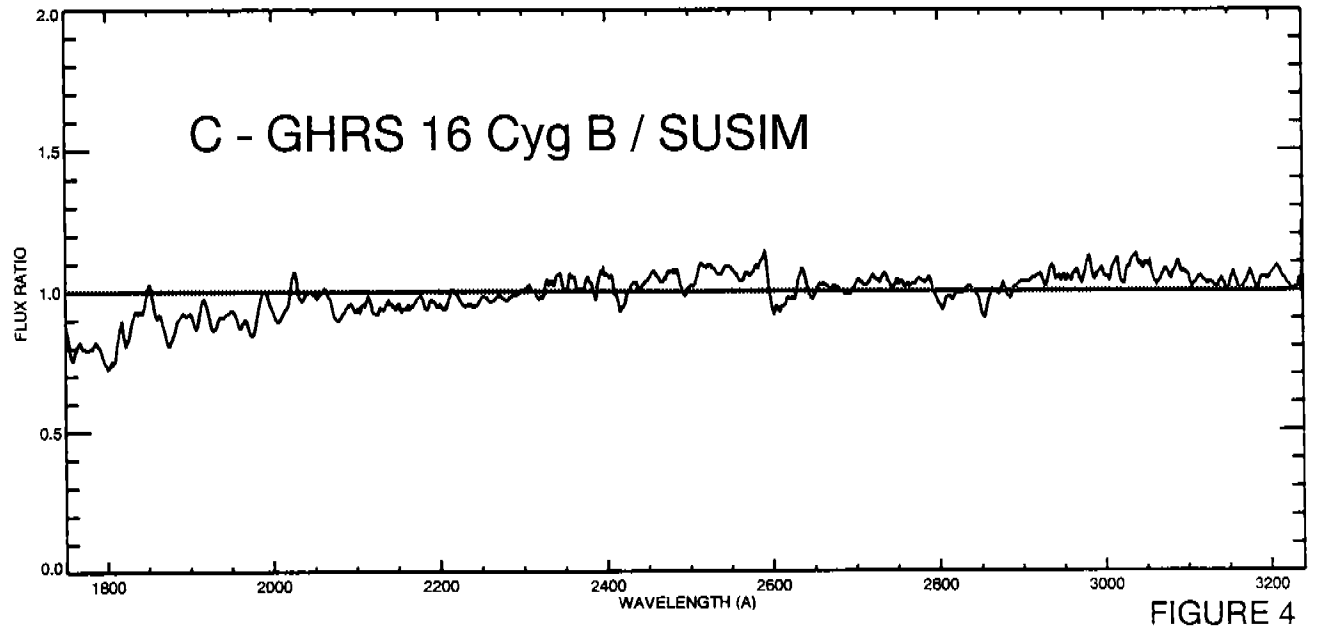
C - GHRS 16 Cyg B / SUSIM
FLUX RATIO
WAVELENGTH (A)
2.0
1.5
1.0
0.5
0.0
1800
2000
2200
2400
2600
2800
3000
3200

FIGURE 4

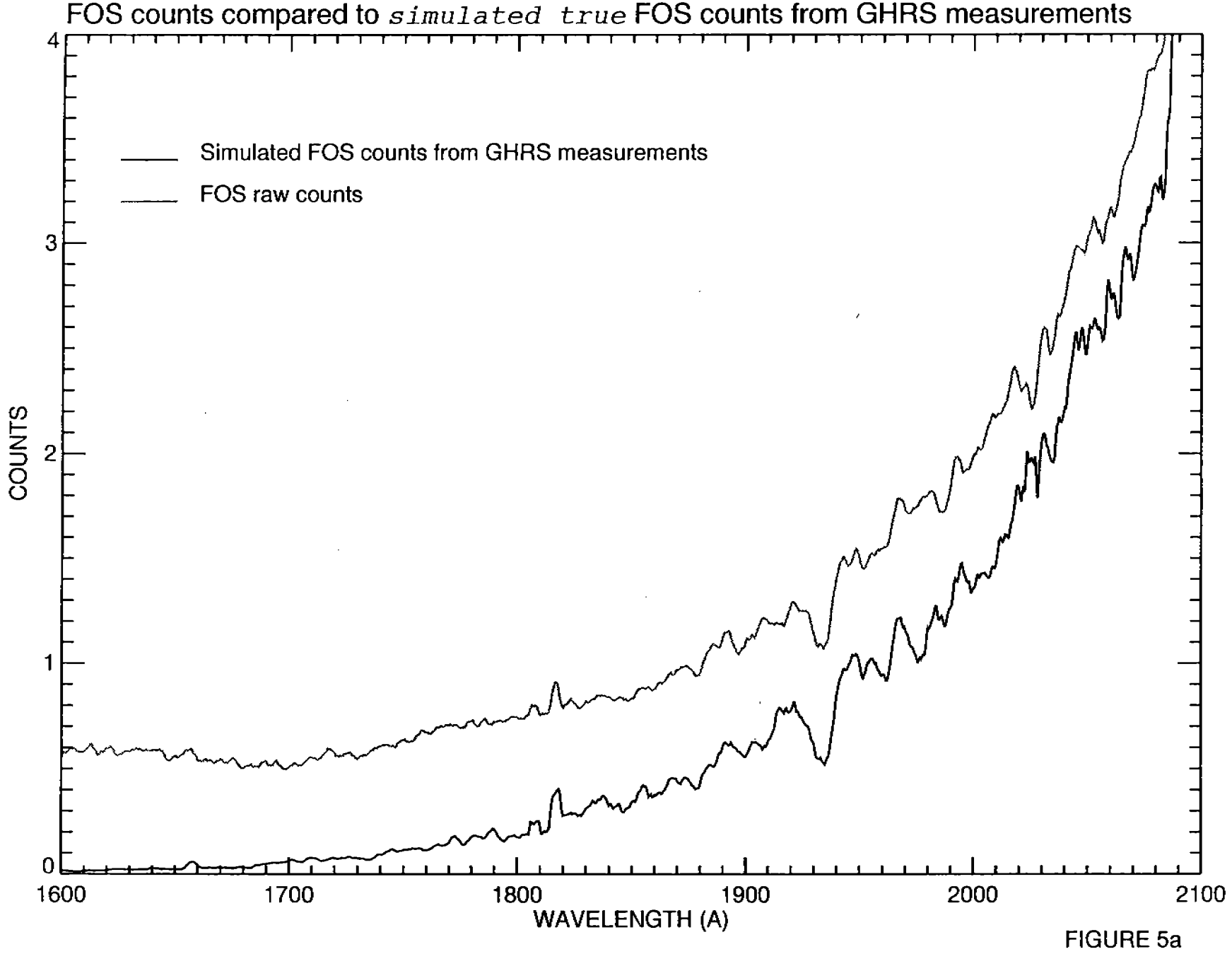
FOS counts compared to simulated true FOS counts from GHRS measurements
Simulated FOS counts from GHRS measurements
FOS raw counts
COUNTS
0
1
2
3
4
1600
1700
1800
1900
2000
2100
WAVELENGTH (A)

FIGURE 5a

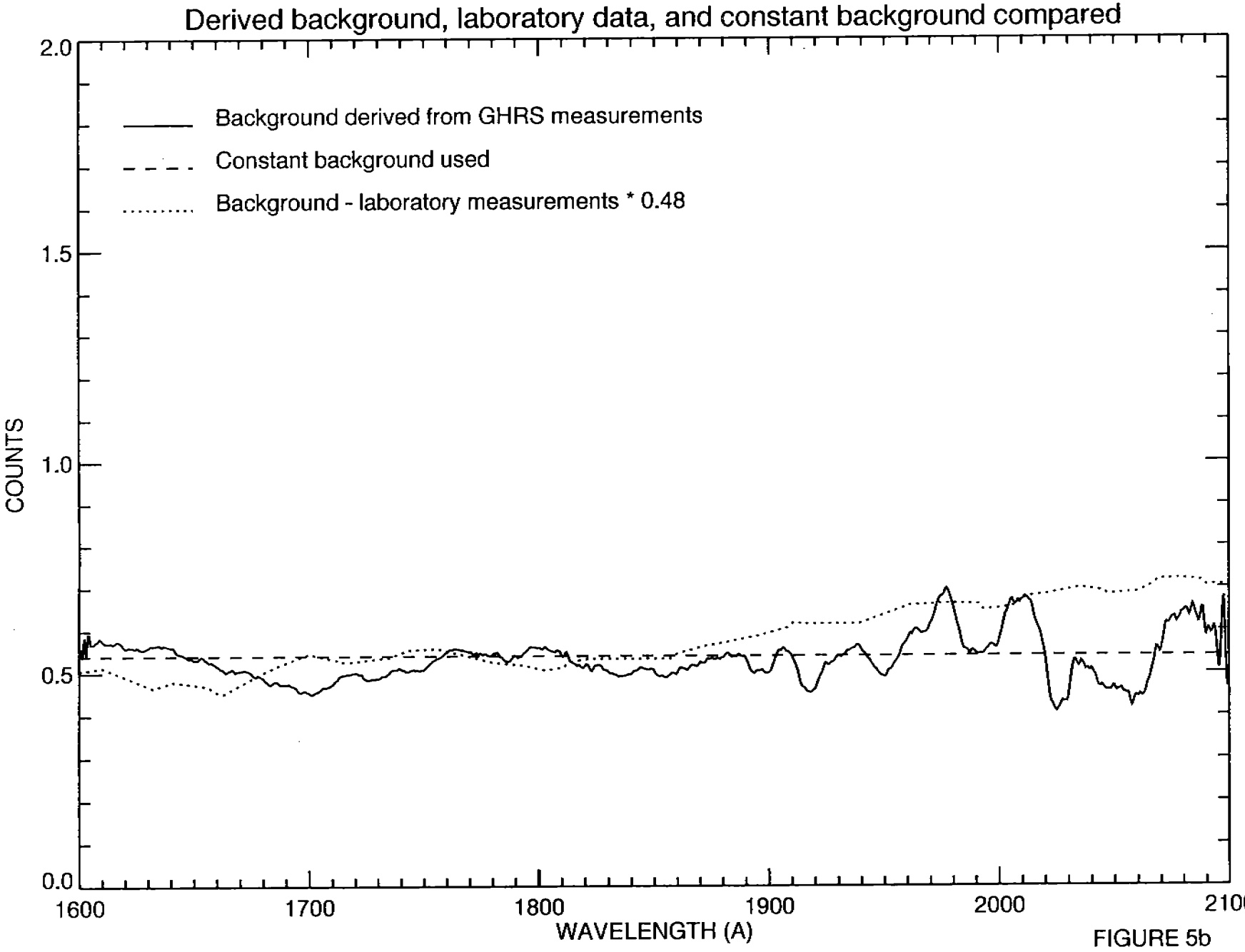
Derived background, laboratory data, and constant background compared
Background derived from GHRS measurements
Constant background used
Background - laboratory measurements * 0.48
COUNTS
2.0
1.5
1.0
0.5
0.0
1600
1700
1800
1900
2000
2100
WAVELENGTH (A)

FIGURE 5b

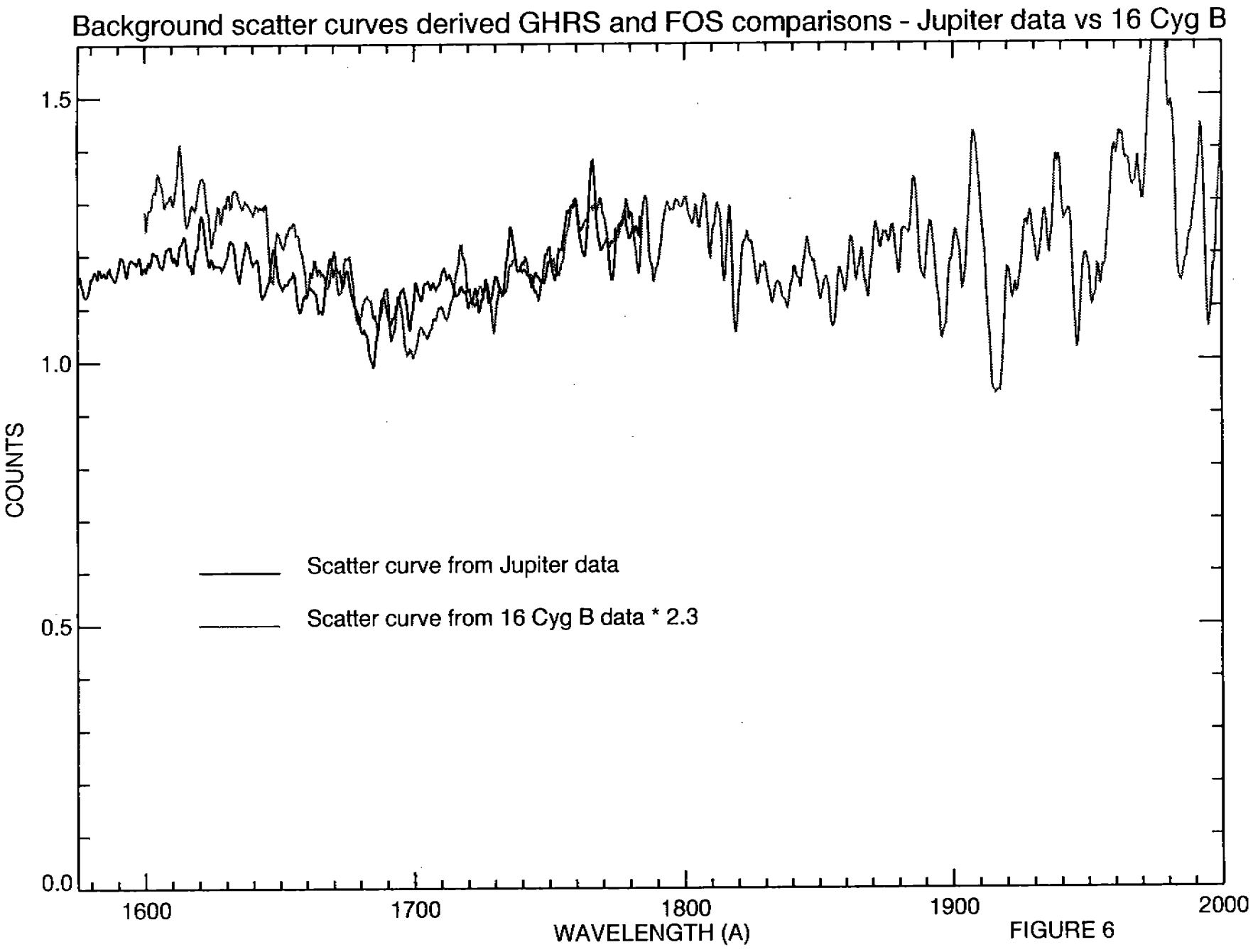
Background scatter curves derived GHRS and FOS comparisons - Jupiter data vs 16 Cyg B
1.5
1.0
0.5
0.0
COUNTS
Scatter curve from Jupiter data
Scatter curve from 16 Cyg B data * 2.3
1600
1700
1800
1900
2000
WAVELENGTH (A)

FIGURE 6

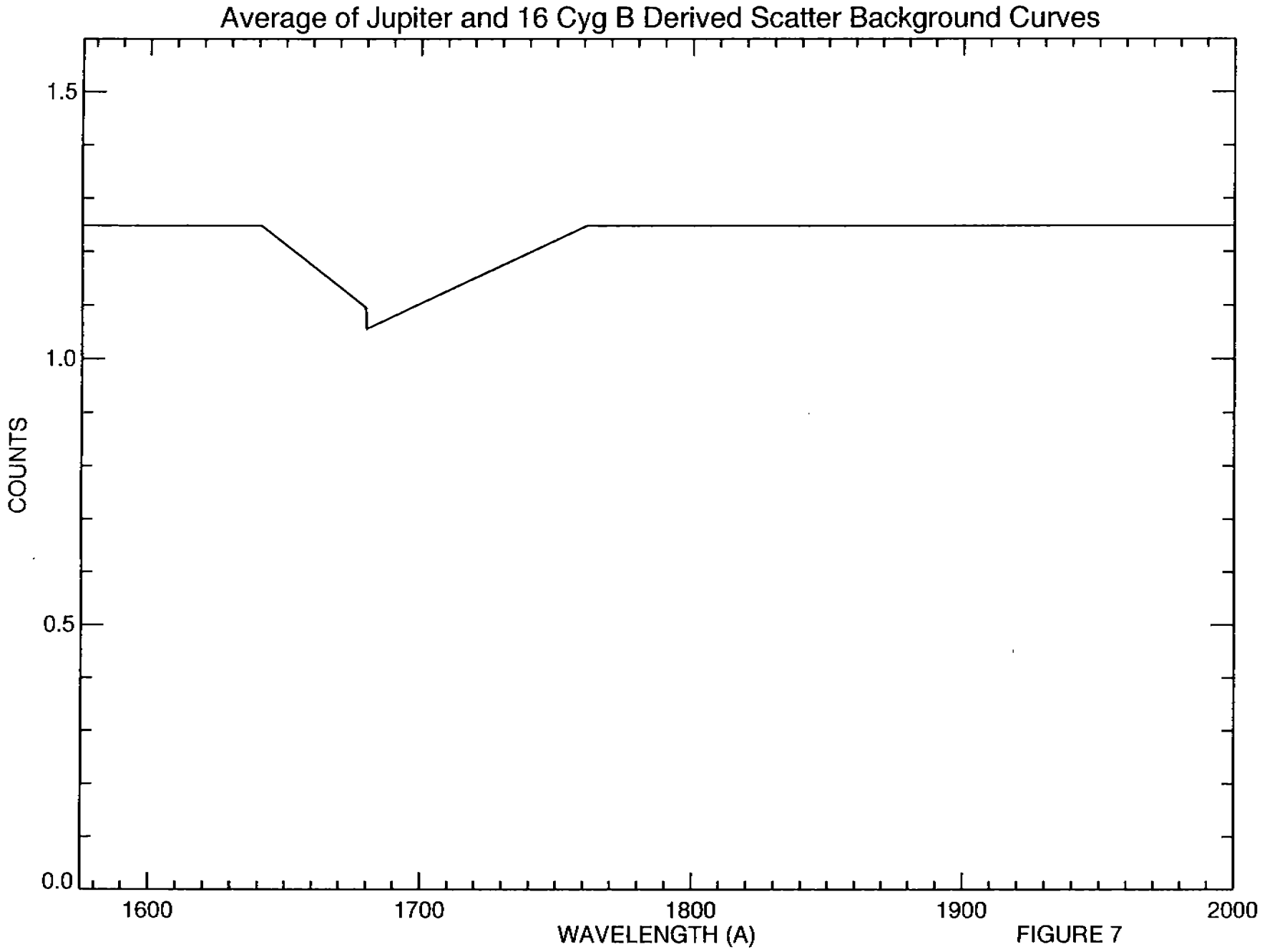
Average of Jupiter and 16 Cyg B Derived Scatter Background Curves
1.5
1.0
0.5
0.0
COUNTS
1600
1700
1800
1900
2000
WAVELENGTH (A)

FIGURE 7